

# Photonic generation of broadly tunable radio-frequency signal using a reflective semiconductor optical amplifier

YOUXI LU<sup>1</sup>, FEI WANG<sup>2\*</sup>, JUN GU<sup>1</sup>, LUN SHI<sup>2</sup>, MENG MENG PENG<sup>1</sup>, JINGXIN HUANG<sup>2</sup>, WEN KANG<sup>2</sup>

<sup>1</sup>Institute of Science, Chongqing University of Technology,  
Chongqing 400054, P.R. China

<sup>2</sup>Institute of Electrical and Electronic Engineering, Chongqing University of Technology,  
Chongqing 400054, P.R. China

\*Corresponding author: wangf17@cqut.edu.cn

A novel scheme for photonic generation of broadly tunable radio frequency signal using a reflective semiconductor optical amplifier (RSOA) is demonstrated. A continuous wave emitted from the laser diode is modulated by a Mach–Zehnder modulator, then the modulated optical carrier is injected into the RSOA. Due to the four-wave mixing effect in the RSOA, the limited frequency components of the modulated signal are expanded, which directly lead to the generation of a wide frequency comb. Two optical tunable bandpass filters are parallelly connected to select the desired sidebands, which are launched into a photodetector or photomixer to generate radio frequency signal by beating. Using the proposed method, the bandwidth of generated radio frequency signal can range from 20 to 300 GHz.

Keywords: radio frequency signal generation, semiconductor optical amplifiers, four-wave mixing.

## 1. Introduction

As the demand for wireless broadband speed, the higher radio frequency (RF) signals become more and more important. Higher RF frequencies can increase the available frequency bandwidth and increase the capacity of a single channel [1]. With the increase of RF signal frequency, the antenna can be small, thus reducing the power consumption of mobile devices. Nowadays, how to generate and transmit high-frequency signals is a problem that needs to be solved urgently [2]. The radio-over-fiber (RoF) technology, combining the advantages of wireless and fiber optics, is a promising one [3, 4]. Compared with electrical methods, optical methods can be immunity to electromagnetic interference, high flexibility, can generate multiples of a reference frequency [3, 5]. Particularly, it can generate signals having a frequency higher than 100 GHz compared to the conventional technique in electrical domain. Optical heterodyning method is

a common method for photonic generation of RF signals. In general, there are two ways based on optical heterodyning to generate RF signals. One is using two lasers cascaded with optical devices for enhancing their phase correlation to generate RF signals. For example, RF signals generation can be achieved by using a monolithic ridge waveguide laser with two digital distributed feedback (DFB) lasers [6] or using a monolithic optical RF generator consisting of two DFB lasers and a semiconductor ring laser (SRL) [3]. And the other is using one laser with external optical modulation to generate RF signals. For example, RF signals can be generated using a Mach–Zehnder modulator (MZM) and a high nonlinear optical fiber HNLF [7], or using a MZM and a semiconductor optical amplifier (SOA) [5] to achieve frequency doubling and generate high frequency RF signal.

In this paper, a novel scheme for photonic generation of broadly tunable RF signals, based on four-wave mixing (FWM) effect in a reflective semiconductor optical amplifier (RSOA), is proposed and demonstrated. In the proposed scheme, the optical carrier modulated by a MZM is injected into a RSOA. Due to the FWM effect in the RSOA, the limited frequency components of the modulated signal are expanded, which lead to the generation of a wide frequency comb. FWM is a phase sensitive process that could lead to power exchange among different sidebands. So, the generated frequency components have phase correlation [3]. Then the two sidebands are filtered out by two parallel optical tunable bandpass filters (OTBFs) with different central wavelengths, and are launched into a photodetector (PD) or photomixer (PX) directly to generate a RF signal by beating. Due to the FWM effect and broad gain band of the RSOA, a wide optical frequency combs (OFC) are generated. The generated RF signals by two different sidebands beating can cover microwave/millimeter-wave, even THz-wave band. We also discussed the influence of the input optical power and the bias voltage of the RSOA on the system performance. Compared with the other methods, this scheme has many unique advantages, such as simple structure, easy tuning and easy integration, and so on.

## 2. Experimental scheme and principle

The schematic diagram of the presented photonic generation scheme for broadly tunable RF signals is shown in Fig. 1. A continuous wave (CW) emitted from the laser diode (LD) is modulated by a MZM driven by a 20-GHz successive sinusoidal electrical signal, whose wavelength locates at 1552.52 nm. Then the modulated optical carrier is injected into the RSOA. The limited frequency components of the modulated signal are expanded because of the FWM effect and broad gain band in the RSOA, and a wide OFC is generated. Using two 50:50 optical couplers (OC), the OFC from the RSOA is divided into two parts, and then is injected into two parallel OTBFs (OTBF1 and OTBF2) with different central frequency, respectively. Two different frequency components are filtered out via the two OTBFs and are launched into a PD or PX. By using the optical heterodyning, the RF signal with the frequency corresponding to the wavelength spacing of two filtered frequency components can be generated.

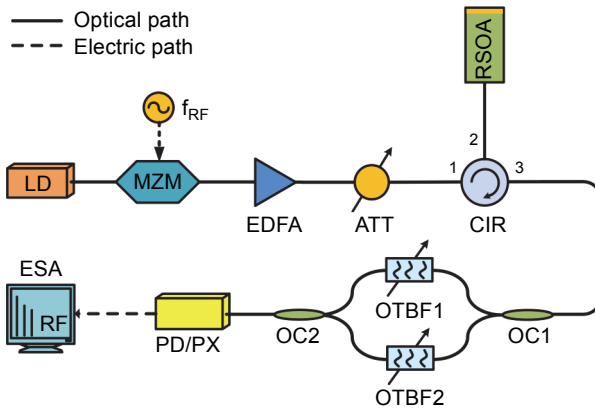


Fig. 1. Schematic of the proposed photonic generation of RF signal; LD – laser diode, EDFA – erbium-doped fiber amplifier, ATT – attenuator, MZM – Mach-Zehnder modulator, CIR – circulator, RSOA – reflective semiconductor optical amplifier, OC – optical coupler, OTBF – optical tunable bandpass filter, PD – photodetector, PX – photomixer, and ESA – electrical spectrum analyzer.

The SOA is known for having variety of optical nonlinear effects, such as the FWM effect. Compared to traveling wave SOA, RSOA has stronger nonlinear effects due to the optical field twice passing through the active region of RSOA [8, 9]. When the modulated signal is launched into RSOA, on the one hand, all the frequency components of the modulated signal are amplified; on the other hand, because of FWM of the RSOA, the limited frequency components of the modulated signal are expanded. The relationship between the newly generated frequency components of FWM and the frequency components of other participating FWM effects can be expressed as follows: when light  $\omega_{p1}$ ,  $\omega_{p2}$  and  $\omega_{probe}$  are injected into the RSOA the new frequency component at the output of the RSOA is the combination of the incident light wave frequencies

$$\omega_{idler} = \omega_{p1} + \omega_{p2} - \omega_{probe}$$

where  $\omega_{idler}$  is the generated optical angular frequency, which is commonly known as “idler”,  $\omega_{p1}$ ,  $\omega_{p2}$  denote angular frequencies of two pump signals, and  $\omega_{probe}$  is angular frequency of probe signal.

Because FWM effect is a phase sensitive process that could lead to power exchange among different sidebands, the newly generated frequency component satisfies the specific phase matching condition with the original frequency component [10]. Therefore, there is a strong phase correlation between the frequency components in OFC.

### 3. Results and discussion

As it is depicted in Fig. 1, CW is emitted by the LD (Yenista Optical, YO14130239), whose wavelength locates at 1552.52 nm, then is modulated in the MZM (Photline MXAN-LN-20) driven by a 20-GHz electrical signal, and the electrical signal is loaded onto the optical carrier. Figure 2 reports the optical spectrum of the modulated optical

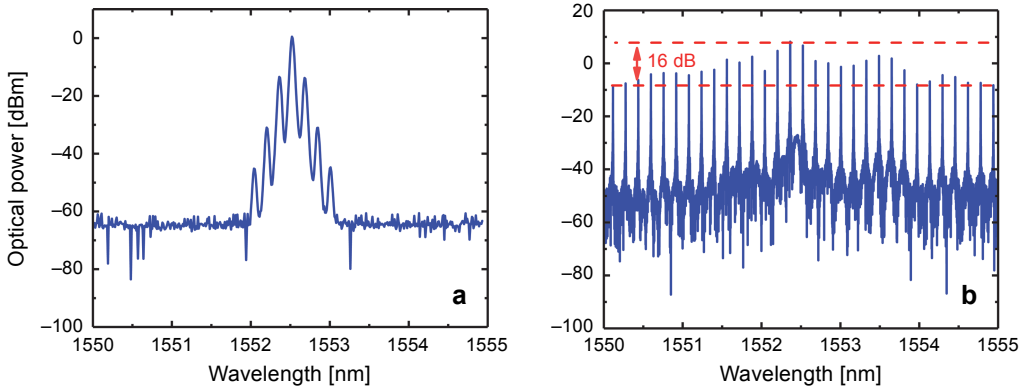


Fig. 2. The optical spectrum of the modulated optical signal before RSOA (a), and the frequency comb output from RSOA (b).

signal before RSOA and the frequency comb output from RSOA, which is detected by an optical spectrum analyzer (OSA, Anritsu MS9740A). As shown in Fig. 2a, the optical spectrum of the modulated optical signal before RSOA only has several orders sidebands. And each sideband has a 20-GHz wavelength interval. As can be seen from Fig. 2b, when the modulated signal is injected into the RSOA, the frequency components of the modulated optical carrier are expanded, and intensity is enhanced. Meanwhile, within a certain wavelength range from 1550 to 1555 nm, the intensity of the sidebands is nearly equivalent. The range of intensity change is less than 16-dB. Using the proposed method, the available bandwidth of generated RF signals has been greatly expanded.

Since the frequency combs with 20-GHz wavelength spacing have been obtained, two narrow band OTBFs are used to filter out the corresponding frequency components.

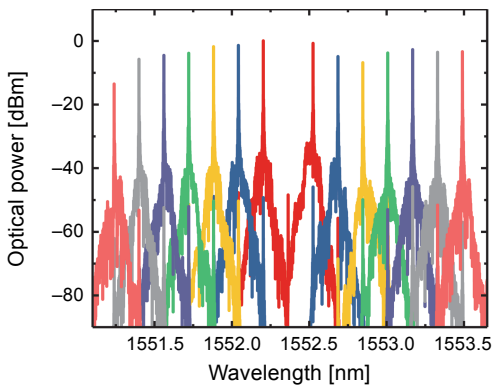


Fig. 3. The optical spectrum of output field after filtering, the wavelength spacing is an integer multiple of 40 GHz.

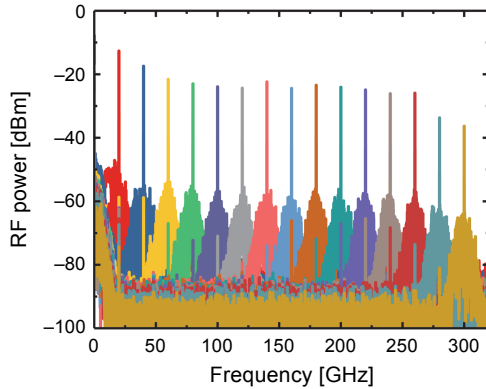


Fig. 4. The electrical spectrum of the RF signal generated by beating in PD/PX, with a span of 20 GHz.

The OTBFs used (OTBF1 and OTBF2) have the same 3-dB bandwidth (10 GHz) and the same filter function (first-order Gaussian shape). The two optical fields through OTBFs were coupled together via OC2, then are launched into a PD or PX to generate a RF signal. Figure 3 shows the output field after filtering, wavelength spacing is an integer multiple of 40 GHz. Figure 4 shows the electrical spectrum of the RF signal generated by beating in PD/PX, which has a span of 20 GHz. Using the proposed scheme, by altering the filter center frequency of two OTBFs, RF signal from 20 to 300 GHz with a span of 20 GHz can be generated. The PD with the bandwidth of up to 120 GHz is commercially available. When the frequency spacing between the two incident waves is larger than 100 GHz, the PD will not respond efficiently to the beating signal, and the power of the generated RF signal may be extremely low. However, this problem can be overcome by using a PX with a bandwidth of up to 3 THz, which is commercially available [5, 11]. In addition, in the proposed scheme, since the generated frequency comb is divided into two branches and two OBPFs are parallelly inserted to select an optical line, respectively, the two optical lines selected by the two optical filters propagate along different optical paths. The optical phase difference between the two lines can be variable, which contributes to phase noise of the generated microwave signal. Concerning this point, which had been investigated using the similar structure in [12], the results showed the high phase stability still can be achieved.

In this scheme, to obtain stable broadly tunable RF signals, the flatness of the OFC is a key factor [13]. A wider, flatter OFC can make it easier to obtain RF signals with good tunable effects [14, 15]. So, next we will discuss the effects of various factors on OFC, such as the input optical power and the bias voltage of the RSOA.

Figure 5 shows the OFC output from RSOA utilizing different input optical power. Figure 5a uses a  $-2$  dBm optical source. The input optical powers of RSOA in the Figs. 5b–5f are 0, 2, 4, 6, and 8 dBm, respectively. And all the bias voltage of the RSOA is 0.8 V. From the diagram we can know that, at less than 6 dBm of the input power

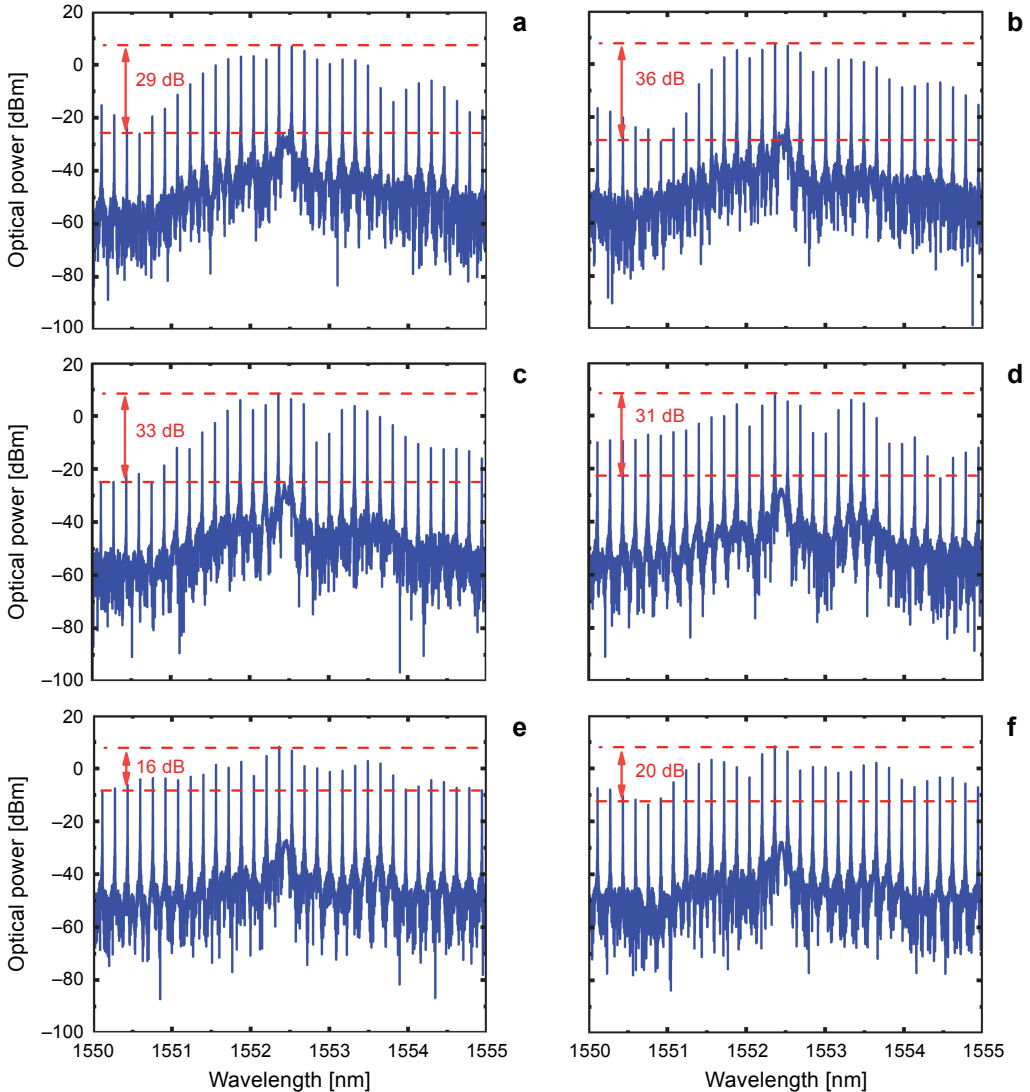


Fig. 5. The frequency comb output from RSOA utilizing different input optical power. The input powers of RSOA are  $-2$  dBm (a),  $0$  dBm (b),  $2$  dBm (c),  $4$  dBm (d),  $6$  dBm (e), and  $8$  dBm (f).

of RSOA, the OFC gradually becomes flat with the increase of optical power. When the optical power is higher than  $6$  dBm, the flatness of the OFC begins to decline. It can be seen from Fig. 5 that when the optical power is around  $6$  dBm, the flatness of the OFC is the best. The spectrum is shown in Fig. 5a. The output spectrum of the OFC with power deviation is  $29$ -dB. In Fig. 5e, when we tune the output power of LD to  $6$  dBm, the power deviation is changed to  $16$ -dB. Furtherly, when we tune the optical power higher than  $6$  dBm, the flatness of the OFC decreases. From this set of diagrams, we can see that the OFC is flatter when the output optical power of LD is around  $6$  dBm.

Not only the input optical power of RSOA can influence the lines of the OFC, the bias voltage also has an influence on OFC. We found that the bias voltage can change the carrier and the effective gain in the RSOA. Ultimately, the gain and nonlinear effects of RSOA are affected. Figure 6 shows the OFC output from RSOA utilizing different bias voltage. The input powers of RSOA in the Figs. 6a–6f are 0.2, 0.4, 0.6, 0.8, 1.0, and 1.2 V, respectively. And all the optical power of the LD is 6 dBm. From Fig. 6 we can know that, when the bias voltage is lower than 0.8 V, the OFC gradually becomes flat with the increase of bias voltage. Such as Fig. 6a, the power fluctuation of

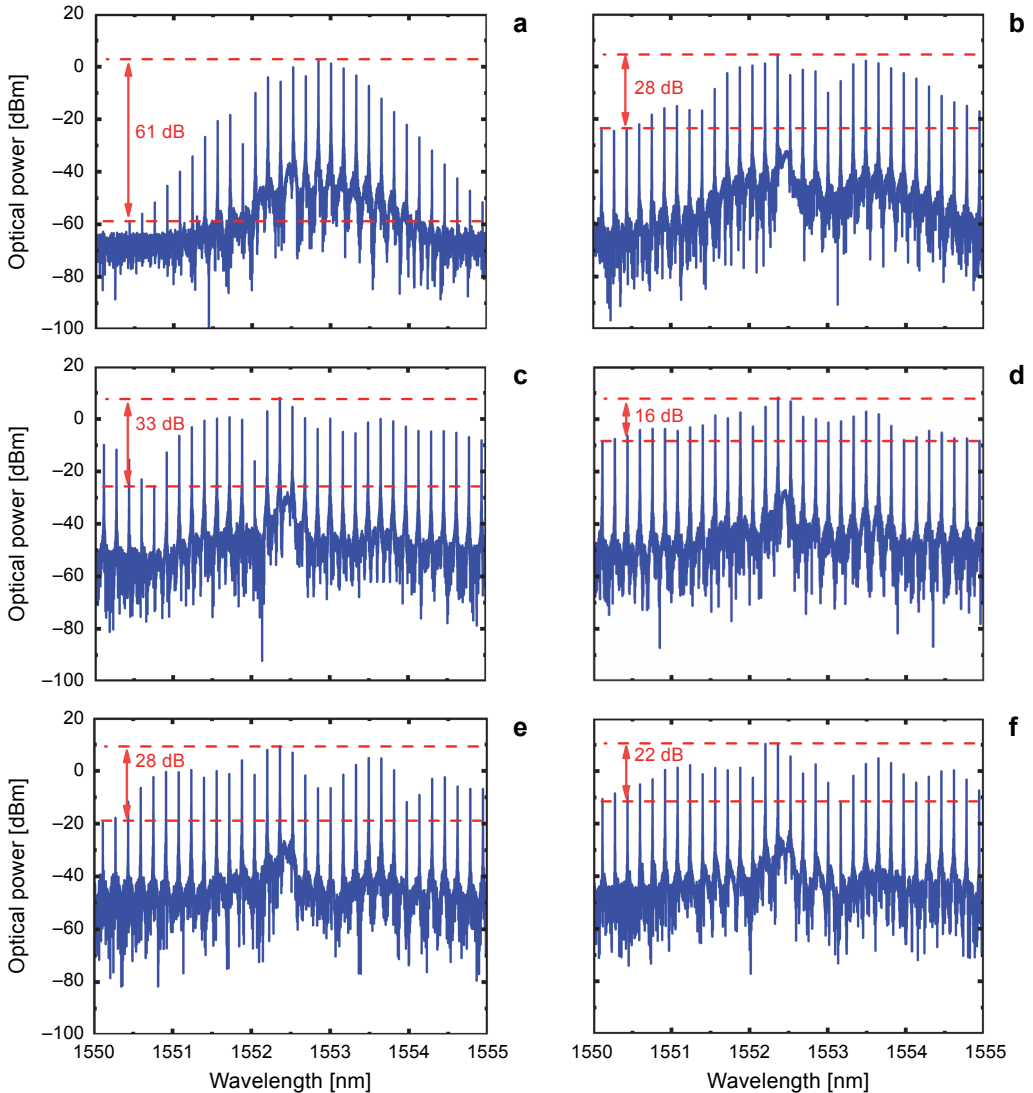


Fig. 6. The frequency comb output from RSOA utilizing different bias voltage. The bias voltages of RSOA are 0.2 V (a), 0.4 V (b), 0.6 V (c), 0.8 V (d), 1.0 V (e), and 1.2 V (f).

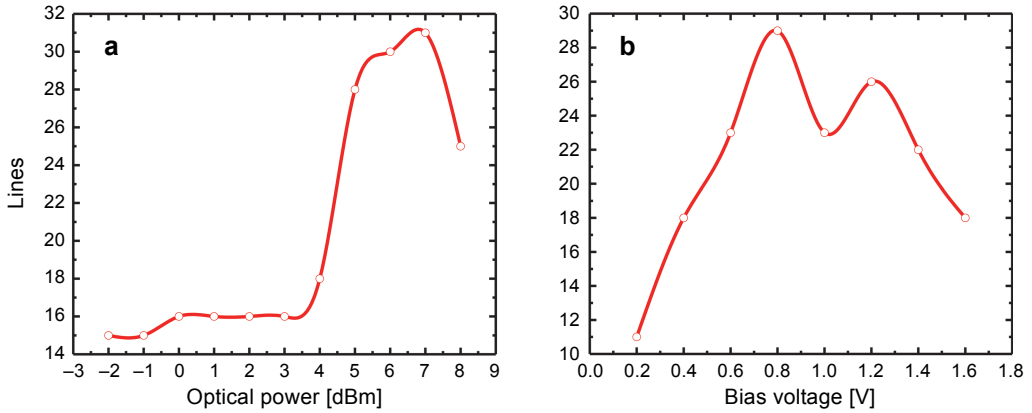


Fig. 7. The OFC for 20-GHz modulated signal. The line number of the OFC vs. the input optical power of the RSOA (the bias voltage is 0.8 V) (a); and the line number of the OFC vs. the bias voltage of the RSOA (the injection optical power is 6 dBm) (b).

OFC output from RSOA is up to 61-dB. When the bias voltage is higher than 0.8 V, the flatness of the OFC begins to decline. It can be learned from this figure that when the bias voltage is around 0.8 V, the flatness of the OFC is the best. In this condition, the output spectrum of the OFC with power deviation is 16-dB.

The flatness of OFC also can be characterized by the line number of effective frequency components within a certain power range. We use a 20-GHz modulated signal, the power variation of frequency components is set within 15 dB. Figure 7a shows the line number of the OFC vs. the input optical power of the RSOA, when input optical power of the RSOA is changed from  $-2$  to 8 dBm, and bias voltage is 0.8 V. As shown in the figure, when the input optical power is around 6 dBm, the number of the lines is the largest. Figure 7b shows the number of the lines of the OFC vs. RSOA's bias voltage range from 0.2 to 1.6 V, and input optical power of RSOA is 6 dBm. As can be seen, the number of the lines of OFC is the largest when the bias voltage is around 0.8 V. Compared with the input optical power, the bias voltage of the RSOA has a greater influence on the flatness of the OFC.

## 4. Conclusions

In this paper, a novel scheme for broadly tunable photonic generation of RF signals based on optical heterodyning using MZM and RSOA is proposed and demonstrated. Due to FWM effect and broad gain band of the RSOA, the limited frequency components of the modulated signal are expanded, a broad frequency comb is generated. By adjusting the central frequency of two OTBFs to filter out corresponding frequency components, and then launching the two filtered lasing wavelengths into a PD/PX, microwave/millimeter-wave or THz-wave can be conveniently obtained. In addition, we also investigated the input optical power and bias voltage of RSOA influence on OFC. When the



input optical power and the bias voltage of RSOA are respectively around 6 dBm and 0.8 V, the generated OFC has a flatness spectrum, which makes for broadly RF signals generation.

*Acknowledgements* – This work was supported by the National Natural Science Foundation of China (61575034), the recruitment program of global experts (WQ20165000357), the Key Project of the Natural Science Foundation Project of Chongqing (cstc2013jjB40002).

## References

- [1] ZHENHUA FENG, BORUI LI, MING TANG, LIN GAN, RUOXU WANG, RUI LIN, ZHILIN XU, SONGNIAN FU, LEI DENG, WEIJUN TONG, SHENGYA LONG, LEI ZHANG, HONGYAN ZHOU, RUI ZHANG, SHUANG LIU, PERRY PING SHUM, *Multicore-fiber-enabled WSDM optical access network with centralized carrier delivery and RSOA-based adaptive modulation*, IEEE Photonics Journal **7**(4), 2015, article ID 7201309, DOI: [10.1109/JPHOT.2015.2445103](https://doi.org/10.1109/JPHOT.2015.2445103).
- [2] YONGHOON CHOI, YOUNGNAM HAN, *Modeling and analysis of millimeter/sub-millimeter wave indoor communications for multi-gigabit wireless transmission*, [In] *2014 39th International Conference on Infrared, Millimeter, and Terahertz waves (IRMMW-THz)*, 2014, pp. 1–2, DOI: [10.1109/IRMMW-THz.2014.6956383](https://doi.org/10.1109/IRMMW-THz.2014.6956383).
- [3] NING ZHANG, XINLUN CAI, SIYUAN YU, *Optical generation of tunable and narrow linewidth radio frequency signal based on mutual locking between integrated semiconductor lasers*, Photonics Research **2**(4), 2014, pp. B11–B17, DOI: [10.1364/PRJ.2.000B11](https://doi.org/10.1364/PRJ.2.000B11).
- [4] ZANOLA M., STRAIN M.J., GIULIANI G., SOREL M., *Monolithically integrated DFB lasers for tunable and narrow linewidth millimeter-wave generation*, IEEE Journal of Selected Topics in Quantum Electronics **19**(4), 2013, article ID 1500406, DOI: [10.1109/JSTQE.2012.2235412](https://doi.org/10.1109/JSTQE.2012.2235412).
- [5] KUMAR A., PRIYE V., *Photonic generation of high frequency millimeter-wave and transmission over optical fiber*, Applied Optics **55**(22), 2016, pp. 5830–5839, DOI: [10.1364/AO.55.005830](https://doi.org/10.1364/AO.55.005830).
- [6] YANG S.-H., WATTS R., LI X., WANG N., COJOCARU V., O’GORMAN J., BARRY L.P., JARRAHI M., *Tunable terahertz wave generation through a bimodal laser diode and plasmonic photomixer*, Optics Express **23**(24), 2015, pp. 31206–31215, DOI: [10.1364/OE.23.031206](https://doi.org/10.1364/OE.23.031206).
- [7] YANG JIANG, PING SHUM, XINWU YANG, MENG JIANG, *Optical millimeter-wave generation utilizing optical parametric loop mirror and fiber Bragg grating*, [In] *2011 Asia Communications and Photonics Conference and Exhibition (ACP)*, 2011, pp. 1–5, DOI: [10.1117/12.905615](https://doi.org/10.1117/12.905615).
- [8] FEI WANG, XIN-LIANG ZHANG, YU YU, XI HUANG, *82-channel multi-wavelength comb generation in a SOA fiber ring laser*, Optics and Laser Technology **42**(2), 2010, pp. 285–288, DOI: [10.1016/j.optlastec.2009.07.006](https://doi.org/10.1016/j.optlastec.2009.07.006).
- [9] ANTONELLI C., MECOZZI A., *Reduced model for the nonlinear response of reflective semiconductor optical amplifiers*, IEEE Photonics Technology Letters **25**(23), 2013, pp. 2243–2246, DOI: [10.1109/LPT.2013.2282215](https://doi.org/10.1109/LPT.2013.2282215).
- [10] CAI X., HO Y.-L.D., MEZOSI G., WANG Z., SOREL M., YU S., *Frequency-domain model of longitudinal mode interaction in semiconductor ring lasers*, IEEE Journal of Quantum Electronics **48**(3), 2012, pp. 406–418, DOI: [10.1109/JQE.2012.2182759](https://doi.org/10.1109/JQE.2012.2182759).
- [11] DENINGER A.J., ROGGENBUCK A., SCHINDLER S., PREU S., *2.75 THz tuning with a triple-DFB laser system at 1550 nm and InGaAs photomixers*, Journal of Infrared, Millimeter, and Terahertz Waves **36**(3), 2015, pp. 269–277, DOI: [10.1007/s10762-014-0125-5](https://doi.org/10.1007/s10762-014-0125-5).
- [12] LOGAN R.T., *All-optical heterodyne RF signal generation using a mode-locked-laser frequency comb: theory and experiments*, [In] *2000 IEEE MTT-S International Microwave Symposium Digest (Cat. No. 00CH37017)*, Vol. 3, 2000, pp. 1741–1744, DOI: [10.1109/MWSYM.2000.862315](https://doi.org/10.1109/MWSYM.2000.862315).

- [13] TING YANG, JIANJI DONG, SHASHA LIAO, DEXIU HUANG, XINLIANG ZHANG, *Comparison analysis of optical frequency comb generation with nonlinear effects in highly nonlinear fibers*, Optics Express **21**(7), 2013, pp. 8508–8520, DOI: [10.1364/OE.21.008508](https://doi.org/10.1364/OE.21.008508).
- [14] DEL'HAYE P., SCHLIESSER A., ARCIZET O., WILKEN T., HOLZWARTH R., KIPPENBERG T.J., *Optical frequency comb generation from a monolithic microresonator*, Nature **450**, 2007, pp. 1214–1217, DOI: [10.1038/nature06401](https://doi.org/10.1038/nature06401).
- [15] FUKUSHIMA S., SILVA C.F.C., MURAMOTO Y., SEEDS A.J., *Optoelectronic millimeter-wave synthesis using an optical frequency comb Generator, optically injection locked lasers, and a unitraveling-carrier photodiode*, Journal of Lightwave Technology **21**(12), 2003, pp. 3043–3051, DOI: [10.1109/JLT.2003.822250](https://doi.org/10.1109/JLT.2003.822250).

*Received January 5, 2018  
in revised form March 23, 2018*